analytical chemistry

pubs.acs.org/ac Article

Antifouling Peptide Hydrogel Based Electrochemical Biosensors for Highly Sensitive Detection of Cancer Biomarker HER2 in Human Serum

Wenqi Wang, Rui Han, Min Chen, and Xiliang Luo*

Cite This: *Anal. Chem.* 2021, 93, 7355−7361 Read Online

ACCESS | Metrics & More | Article Recommendations | Supporting Information

ABSTRACT: A facile strategy for the electrochemical detection of human epidermal growth factor receptor 2 (HER2), a breast cancer biomarker, was presented via the fabrication of an antifouling sensing interface based on the conducting polymer poly(3,4-ethylenedioxythiophene) (PEDOT) and a biocompatible peptide hydrogel. The peptide hydrogel prepared from a designed short peptide of Phe-Glu-Lys-Phe functionalized with a fluorene methoxycarbonyl group (Fmoc-FEKF) enabled excellent activity preservation for the immobilized biomolecules, and its good hydrophilicity facilitated effective alleviation of nonspecific adsorption or biofouling, while the PEDOT film provided a highly stable and conducting substrate. The developed biosensor was highly sensitive and selective for HER2 detection, with a wide linear response range from 0.1 ng mL^{-1} to 1.0 μg mL^{-1} and a low limit of detection of 45 pg mL^{-1}. Moreover, the peptide hydrogel based biosensor was feasible to use for complex biological samples, and it was capable of detecting HER2 in human serum with clinically acceptable accuracy, manifesting a promising potential for practical application.

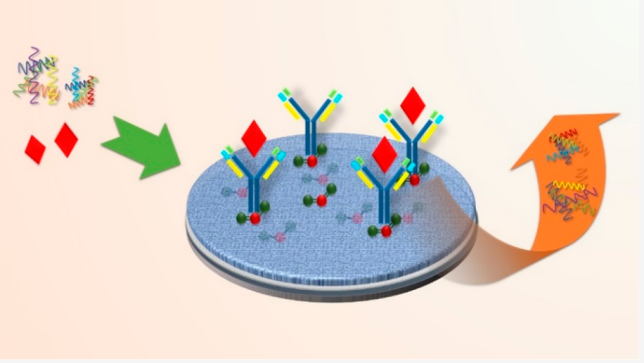

Currently, the early diagnosis of diseases has attracted more and more attention, and numerous assaying methods based on acknowledged biomarkers of a range of human diseases have sprung up.[1−3] Among the present analysis methods, electrochemical immunosensors have gained wide interest due to its high sensitivity, rapid detection, and low cost.[4,5] However, biofouling of the sensing interfaces has posed a serious challenge in practical applications, which would block the electrochemically available surface of electrodes and cause a sequence of adverse effects for analysis in complex biological environments, such as low sensitivity, long response time, and low accuracy of the biosensor in quantifying analytes.[6−8] Consequently, the exploitation of antifouling biosensors that are able to availably resist nonspecific adsorption in complex biological samples has been deemed essential.

To this end, various immunosensing platforms have been constructed via the integration of low-fouling chemistry into the sensing interfaces,[9,10] utilizing diverse materials, such as polymers, zwitterionic materials, peptides, peptoids, and so forth,[11−16] which have been certified to perform efficiently in complex media such as serum and urine and for *in vitro* detection. However, extra constraints such as stability, toxicity, and biocompatibility must be taken into consideration for immunosensor fabrication.[17] Recently, poly(ethylene glycol) (PEG) and its derivatives,[18,19] bovine serum albumin (BSA),[20] hyaluronic acid (HA),[21] 6-mercaptohexanol (MCH),[22] and branched or linear peptides have been introduced to biosensing interfaces to reduce the fouling effects.[12,23,24] Although these materials are harmless and can form antifouling layers on sensing interfaces, few of them are sufficient to form a preeminent biocompatible environment to maintain the immobilized biological molecules with high bioactivity and at the same time exhibit excellent antifouling capability and stability. Therefore, antifouling materials with enhanced biocompatibility and stability remain to be highly required.

Peptide hydrogels have gained popularity in recent years as three-dimensional (3D) porous materials due to their excellent biocompatibility and physical resemblance to biotissues, possessing broad biomedical applications, especially in biosensing, drug carriers, cell culture, and tissue engineering.[25−28] Nonrigid peptide hydrogels with large specific surface areas would reduce steric hindrance and enhance the biomolecule immobilization and target binding. In addition,

Received: March 30, 2021
Accepted: April 28, 2021
Published: May 6, 2021

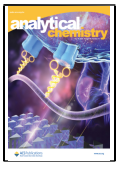

https://doi.org/10.1021/acs.analchem.1c01350
Anal. Chem. 2021, 93, 7355−7361

Scheme 1. Schematic Description of the Fabrication Process of the PEDOT/Peptide Hydrogel Based HER2 Sensor

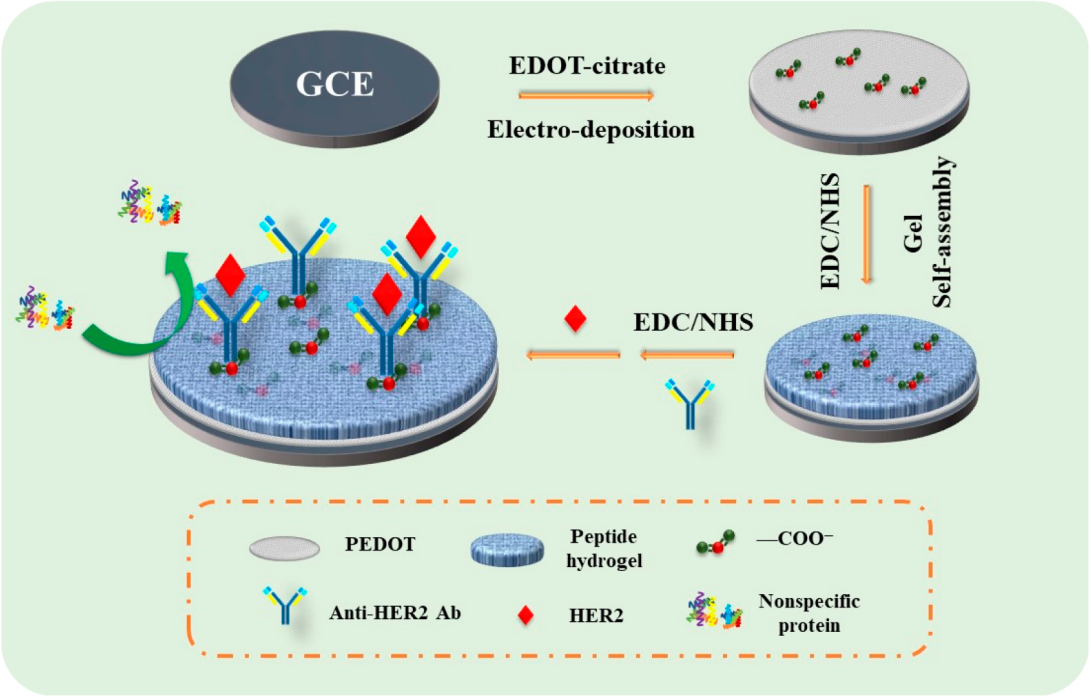

their biocompatible cross-linked networks effectively maintain the activity and intrinsic framework of the connected biomolecules.[29−31] Remarkably, the great hydrophilicity of hydrogels facilitates the formation of hydration layers to alleviate nonspecific macromolecule adhesion onto interfaces, which contributes to their potential utilization in low-fouling biosensors.[32,33] To the best of our knowledge, few reports have explored the utilization of peptide hydrogels as antifouling materials toward the detection of biomarkers in immunosensors.

In this work, peptide hydrogels were employed as a low-fouling biomaterial, and in combination with the conducting polymer poly(3,4-ethylenedioxythiophene) (PEDOT), an electrochemical biosensor for the detection of human epidermal growth factor receptor 2 (HER2) was fabricated, as displayed in Scheme 1. HER2 overexpression has been proved to be associated with the progression of 20−30% of breast cancer tumors.[34] It is demonstrated that raised serum HER2 levels are related to metastatic breast cancer and adverse reactions to chemotherapy and hormonotherapy.[35] Thus, the early detection of HER2 is of great significance for the early diagnosis and treatment of cancer.[36] Conducting polymers, due to their outstanding electronic conductivity, low-cost fabrication, and high stability, have been recognized to be ideal materials as substrates for electrochemical biosensors.[37−39] Herein, the conducting polymer PEDOT was envisaged to provide a stable conductive support and compensate for the poor conductivity of peptide hydrogels to achieve a high sensitivity for HER2 detection. Meanwhile, the hydrogel served as an antifouling interface and matrix for anti-HER2 antibody (Ab) immobilization, alleviated nonspecific protein adsorption, and established a biocompatible environment for immobilized biomolecules to retain high bioactivity. As expected, the constructed HER2 biosensor was low-fouling and highly sensitive, and it was capable of detecting HER2 in complex human serum.

EXPERIMENTAL SECTION

Reagents. A self-designed peptide of Phe-Glu-Lys-Phe functionalized with a fluorene methoxycarbonyl group in the N-terminal (Fmoc-FEKF) was obtained from Bankpeptide Biological Technology Co., Ltd. (Hefei, China), and the structural formula of the designed peptide is shown in Figure S1. Dimethyl sulfoxide (DMSO) was purchased from Sangon Biotech Co., Ltd. (Shanghai, China). Anti-HER2 Ab, HER2, horseradish peroxidase (HRP), and 3,3′,5,5′-tetramethylbenzidine (TMB) were purchased from Beijing Solarbio Science & Technology Co., Ltd. (Beijing, China). 3,4-Ethylenedioxythiophene (EDOT), sodium citrate, 1-ethyl-3-(3dimethylaminopropyl)carbodiimide (EDC), and *N*-hydroxysuccinimide (NHS) were obtained from Aladdin Reagents (Shanghai, China). Myoglobin (Mb) was obtained from Shanghai Titan Scientific Co., Ltd. (Shanghai, China). Lysozyme (LYS), bovine serum albumin (BSA), and fluorescein isothiocyanate-labeled BSA (FITC-BSA) were purchased from Adamas-beta Reagent (Shanghai, China). Immunoglobulin G (IgG), immunoglobulin M (IgM), and human serum albumin (HSA) were purchased from Sigma-Aldrich (Shanghai, China). Carcinoembryonic antigen (CEA) and alpha fetoprotein (AFP) were obtained from Beijing Bo Yang Hongda Technology Co., Ltd. (Beijing, China). The human HER2 ELISA kit was purchased from Meimian Industrial Co., Ltd. (Jiangsu, China). Human serum samples were provided by the Eighth People's Hospital of Qingdao (Qingdao, China). All of the sample preparations were authorized by the institutional review board of the hospital and were performed according to the institutional guidelines and relevant laws. Other reagents were of analytical grade. Millipore water produced by a Milli-Q water purification system (18 MΩ/cm) was used throughout.

Apparatus. Electrochemical experiments were performed using an electrochemical workstation (CHI 760D, Shanghai Chenhua Instrument Co., Ltd., China). The three-electrode

https://doi.org/10.1021/acs.analchem.1c01350
Anal. Chem. 2021, 93, 7355−7361

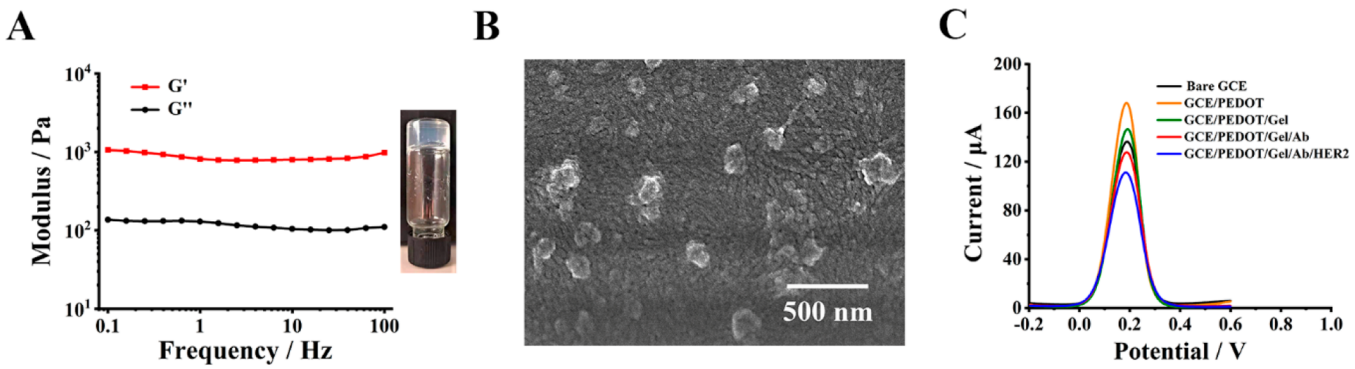

Figure 1. (A) Rheological measurement and a picture of the prepared peptide hydrogel. (B) SEM image of the PEDOT/gel-modified electrode. (C) DPV responses of various electrodes obtained in PBS (10 mM, pH 7.4) containing 5.0 mM $[Fe(CN)_6]^{3-/4-}$ and 0.1 M KCl.

system consisted of a glassy-carbon electrode (GCE), a platinum wire electrode, and a saturated calomel electrode (SCE). Differential pulse voltammetry (DPV) measurements were performed within a potential range of −0.2 to +0.6 V, with an amplitude of 50 mV. Cyclic voltammetry (CV) measurements were performed with a scan rate of 100 mV s^{-1} and a potential from −0.2 to +0.6 V. Both DPV and CV measurements were performed in phosphate-buffered saline solution (PBS, 10 mM, pH 7.4) containing 0.1 M KCl and 5.0 mM $[Fe(CN)_6]^{3-/4-}$.

Scanning electron microscopy (SEM) characterizations were performed with a JEOL JSM-7500F SEM instrument (Hitachi High-Technology Co., Ltd., Japan). Hydrophilicity characterizations of the modified electrode surfaces were performed with a JC2000D1 Instrument (Shanghai Zhongchen Instrument Co., China). An ultraviolet−visible (UV−vis) spectrophotometer (Shimadzu, Japan) was utilized for the measurement of UV−vis spectra. The confocal images were recorded with a TCS SP5 II laser scanning confocal microscope (Leica, Germany).

Preparation of the Peptide Hydrogels. For the preparation of peptide hydrogels, peptide Fmoc-FEKF lyophilized powders were dissolved in DMSO to obtain a Fmoc-FEKF stock solution. After that, the hydrogels were prepared by dilution with Millipore water to a concentration of 5 mg mL^{-1}.[40]

Enzymatic Activity Assay. To assess the enzyme activity, peptide hydrogels that encapsulate HRP were formed by diluting the peptide stock solutions with an aqueous HRP solution (50 μg mL^{-1}), and 20 μL of hydrogels was placed in the 96-well plates. Afterward, 50 μL of hydrogen peroxide and 50 μL of TMB solution (0.3 mg mL^{-1}) were added to the plate successively, and then the mix was incubated at 37 °C. Eventually, 50 μL of 2.0 M H_2SO_4 was added to terminate the enzymatic reaction. The absorbance at 450 nm of the solution was recorded every 5 min. Free HRP and peptide hydrogels without HRP were used as controls.

Preparation of the Antifouling Interface. The construction process of the PEDOT/gel interface is displayed in Scheme 1. Before modification, the bare GCE was initially polished with Al_2O_3 powder and then bathed with absolute ethanol and Millipore water under ultrasonication for about 3 min, respectively. The PEDOT films were synthesized on the bare GCE surfaces by a potentiostatic method with 5.0 mL of an electrodeposition solution containing 0.02 M EDOT and 0.0434 g of sodium citrate, with a 1.1 V constant potential for 200 s. Then, the modified electrodes were soaked in PBS (10 mM, pH 7.4) for 12 h to remove impurities from the electrode surfaces. Afterward, the carboxylic groups of the doped citrate were activated through immersing the PEDOT-modified electrode into PBS containing 0.4 M EDC and 0.1 M NHS for 0.5 h. Then 5.0 μL of Fmoc-FEKF hydrogel was dropped on the electrode surface and incubated for 2 h. After lyophilization, a GCE/PEDOT/gel interface with antifouling ability was obtained.

Fluorescence Characterization. Laser scanning confocal microscopy was utilized to examine the adsorption resistance performance of the GCE/PEDOT/gel interface by visualizing the FITC-BSA adsorbed on different electrode surfaces. Bare GCE and PEDOT-modified electrodes were taken as controls. The electrodes were immersed into a 2.0 mg mL^{-1} FITC-BSA solution for 2 h. After the electrodes were completely washed with Millipore water, electrode surface imaging was performed by confocal microscopy with 488 nm excitation wavelength.

Immobilization of the HER2 Antibody. First, the PEDOT/gel-modified electrode was soaked in PBS (10 mM, pH 7.4) for 0.5 h to achieve an equilibrium swelling state of the hydrogel matrix and then pretreated with CV in PBS (10 mM, pH 7.4), until a stable CV signal was recorded. After that, the carboxylic groups of hydrogels on the GCE/PEDOT/gel were activated with EDC/NHS and then incubated with anti-HER2 Ab at 37 °C, to immobilize the Ab onto the GCE/PEDOT/gel. As a result, a stable biosensor (GCE/PEDOT/Gel/Ab) was prepared.

Detection of HER2. For the detection of targets, HER2 samples with a series of concentrations in PBS (10 mM, pH 7.4) were prepared. The biosensor was incubated with HER2 solutions at 37 °C for 60 min and then washed with PBS and Millipore water. The reduction signals of the biosensor before and after antibody−antigen combination were recorded by DPV.

RESULTS AND DISCUSSION

Characterization of the Peptide Hydrogels. The nearly transparent peptide hydrogels were viscoelastic and solidlike, as was obviously shown in rheological measurements (Figure 1A). A sweep-frequency test of peptide hydrogels revealed a storage modulus (G') significantly higher than the loss modulus (G'') by nearly 1 order of magnitude, testifying to the successful preparation of elastic hydrogels. As characterized by SEM, peptide hydrogels self-assembled into a fibrouslike microstructure, organizing a dense supramolecular meshwork (Figure S2A). Moreover, as hydrogels formed, forces such as β-

https://doi.org/10.1021/acs.analchem.1c01350
Anal. Chem. 2021, 93, 7355−7361

sheet, $\pi-\pi$ stacking, and hydrogen bonds were observed within the peptide hydrogels, as described in our previous work.[41]

Investigation of the Biosensing Interfaces. SEM was used to represent the micromorphology of PEDOT- and PEDOT/gel-modified electrodes. As shown in Figure S2B, after electrodeposition of the PEDOT film on a GCE, a rough but relatively homogeneous surface that was composed of particles was observed. With further modification of the hydrogels, there was a noticeable difference in substrate surface morphology, and the nanofibers of peptide hydrogels covered the surface to form a dense fibrous network (Figure 1B), which could contribute to the formation of a hydration layer to resist the nonspecific adsorption.

The HER2 biosensor assembly process (Scheme 1) was monitored via DPV to characterize changes in the current signal for each procedure of the sensor construction (Figure 1C). After PEDOT film electrodeposition, the oxidation peak current signal was distinctly increased in comparison with that of the bare GCE, mainly due to the PEDOT film having a large surface area and excellent electrical conductivity, which could significantly increase the current and surpass the effect of the carboxyl groups on the surface of the GCE/PEDOT that would repel $[Fe(CN)_6]^{3-/4-}$ and lead to a decrease in the current. Afterward, a significantly reduced current signal was observed due to the modification of the peptide hydrogel, because of the formation of a poorly conducting stratum. Subsequent immobilization of Ab and the specific binding of the HER2 target caused a further decrease of the current signal, respectively, as the formation of antibody−antigen immune complexes caused the sensing surface to be occupied by the dielectric biomolecules, which blocked the electron transfer and induced a decrease in the peak current. Certainly, on the basis of the DPV current signal reduction along with the HER2 target binding, a biosensor for quantitative analysis of HER2 was constructed.

Evaluation of Peptide Hydrogels for Biomolecular Activity Retainability. The designed peptide hydrogels with a fibrous microstructure could form a biocompatible network, which enabled the activity for the immobilized biomolecules to be retained.[31] For verification, an experiment was carried out based on the HRP/TMB chromogenic system by comparing the catalytic properties of the enzyme encapsulated in hydrogels (Gel-HRP) and the free enzyme (HRP). The HRP catalyzed peroxide to oxidize TMB, a chromogenic reagent, to the oxidation state, and then a color change occurred. Therefore, the enzymatic reaction could be observed by monitoring the absorbance of the mixed system. As shown in Figure 2A, the color intensity of the Gel-HRP system was visibly deeper than that of the free HRP system under identical conditions, with an enhanced absorbance at 450 nm after 0.5 h reaction. The pure hydrogels without HRP showed no catalytic capacity to peroxide. Additionally, the catalytic velocity of the Gel-HRP system was clearly higher than that of the free HRP system (Figure 2B). Hence, the catalytic performance of the enzyme encapsulated in hydrogels was dramatically higher than that of the free enzyme, demonstrating that the peptide hydrogel network can provide a biocompatible microenvironment for the biomolecules to retain high bioactivity.

Antifouling Performance. The hydration force was vital for evaluating the protein-repelling capability of a surface. The hydrophilic surfaces possessed preferable ability to inhibit nonspecific adsorption due to their capacity for tightly bonding with water molecules, facilitating formation of the hydration

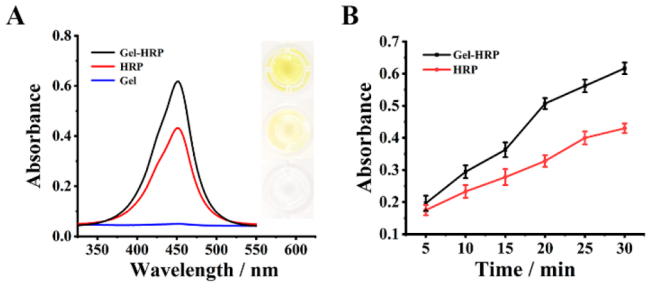

Figure 2. (A) UV−vis spectra and photos (inset) of the chromogenic reaction of the Gel-HRP and free HRP toward peroxide in the presence of TMB after 0.5 h of eaction. (B) Corresponding time−absorbance curves of different reaction systems. Error bars show the standard deviations of three repeated measurements.

layer, which created a barrier to resist biological macromolecules adhesion on surfaces.[42] Herein, the static water contact angles of the bare GCE and PEDOT- and PEDOT/hydrogel-modified electrodes were tested to explore the hydrophilicity of different surfaces (Figure 3A and Table

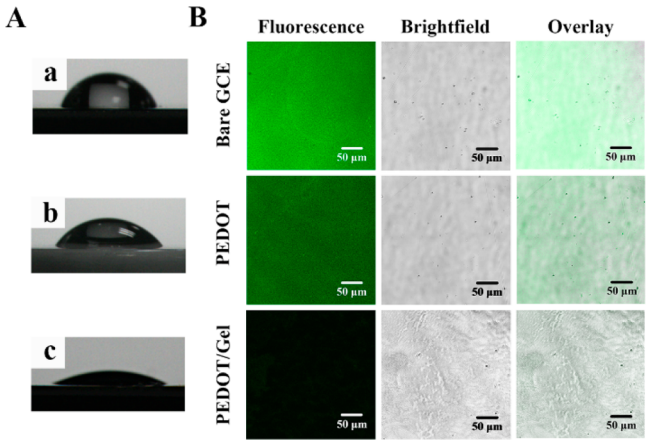

Figure 3. (A) Contact angle characterization of (a) bare, (b) PEDOT-modified, and (c) PEDOT/gel-modified GCEs. (B) Fluorescence images of FITC-BSA-treated bare GCE and PEDOT- and PEDOT/gel-modified surfaces.

S1). The static water contact angle of the GCE/PEDOT/gel surface was 25.00 ± 0.79° (n = 3), relatively smaller than that of the bare GCE (64.03 ± 1.32°, n = 3) and PEDOT surface (56.24 ± 1.41°, n = 3), indicating the excellent hydrophilicity of the PEDOT/hydrogel-modified surface.

Meanwhile, confocal microscopy was utilized to visually examine the ability of the peptide hydrogel modified surface to resist nonspecific protein adsorption by observing the FITC-BSA adsorbed on different surfaces (Figure 3B). Clearly, more protein was absorbed onto the bare GCE and PEDOT-coated electrode, corresponding to a stronger fluorescence of FITC-BSA. In contrast, the fluorescence on the hydrogel-modified GCE surfaces was not evident. It is widely known that protein nonspecific adsorption is primarily governed by hydrophobic interactions in solution systems.[43,44] Therefore, the smaller amount of adsorbed protein may be ascribed to the excellent hydrophilicity of the GCE/PEDOT/gel surface.

To further explore the antifouling ability of different surfaces, DPV was used to monitor the nonspecific protein adsorption using three proteins, Lys (positively charged), Mb

https://doi.org/10.1021/acs.analchem.1c01350
Anal. Chem. 2021, 93, 7355−7361

(neutrally charged), and BSA (negatively charged). As exhibited in Figure 4, the peak current changes of the

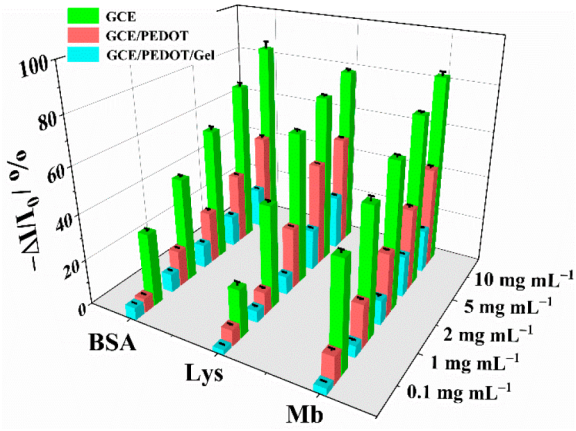

Figure 4. Response changes of the GCE, GCE/PEDOT, and GCE/PEDOT/gel in different protein solutions. The current signal change rate was denoted by $(\Delta I/I_0)/\%$, with the equation $\Delta I = I - I_0$, where I_0 and I refer to the peak currents before and after incubation in protein solutions. Error bars show the standard deviations of three repeated measurements.

PEDOT/gel-modified electrode after incubation in protein solutions with different concentrations were the lowest in comparison with the bare GCE and PEDOT-film-modified electrodes, indicating a prime antifouling ability. Additionally, a comparable antifouling performance of the hydrogel-modified electrode was also reflected in complex serum. As can be seen in Figure 5, the peptide hydrogel based surface mostly maintained the original signal with merely a small decrease (<5% after incubation in 5% human serum). Notably, even for the prepared biosensor binding with the target HER2, the current signal of the GCE/PEDOT/Gel/Ab/HER2 surface still sustained a low rate of change. The antifouling property of the biosensor over 5 h in 5% human serum was also studied, and the results were acceptable (Figure S3). These results obviously testified that the developed PEDOT/gel-modified surface exhibited wonderful antifouling ability in a complex biological environment.

Detection of Biomarker HER2. After the experimental conditions were optimized (Figure S4), an appraisal of the sensor response to HER2 was performed. As shown in Figure 6A, the biosensor response to HER2 was monitored. The current signal decreased with an increase in HER2 concentration, as the specifically attached HER2 to the sensing interface impeded the electron transfer. Good linearity between the DPV signal change rate and the logarithm of the HER2 concentration in the range of 0.1 ng mL^{-1} to 1.0 μg mL^{-1} was obtained, with a linear regression equation of ΔI (μA) = 4.499 log C + 6.304 (R^2 = 0.994) (Figure 6B). The limit of detection (LOD) of the biosensor of 45 pg mL^{-1} (S/N = 3) was much lower than those of many reported assays for HER2 detection (Table S2), which may be attributed to the substrate comprised of PEDOT and peptide hydrogel with a high surface area and excellent biocompatibility, which produced sensitive electrochemical signals and provided a biocompatible environment for the immobilized antibody.

Selectivity, Stability, and Reproducibility of the HER2 Biosensor. To explore the selectivity of the biosensor, a few proteins that may coexist with HER2 in human serum, including IgG, IgM, CEA, AFP, HSA, and a mixture (Mix) of all these proteins, were tested. As displayed in Figure 6C, even at concentrations 100 times greater than that of HER2, these proteins only generated very low signals in comparison with that of the target HER2, indicating the excellent specificity of the biosensor.

Successive CV scans for 50 cycles were conducted to test the stability of the biosensor (Figure S5A). The peak potential and current signal remained almost unchanged. Additionally, the biosensor displayed a retention of >90% of the original signal after being stored in PBS (10 mM, pH 7.4) for up to 15 days (Figure S5B). The reproducibility was assessed by detecting 1.0 μg mL^{-1} HER2 using five independently fabricated biosensors. The relative standard deviation was 5.44% (Figure S5C), justifying acceptable reproducibility.

Clinical Application for HER2 Detection in Serum Samples. To evaluate the feasible clinical utility of the developed biosensor, serum samples of five breast cancer patients were analyzed. A commercial ELISA kit was used as a control to detect the same samples. As can be seen in Figure 6D, the results exhibited fine correlation of the two methods.

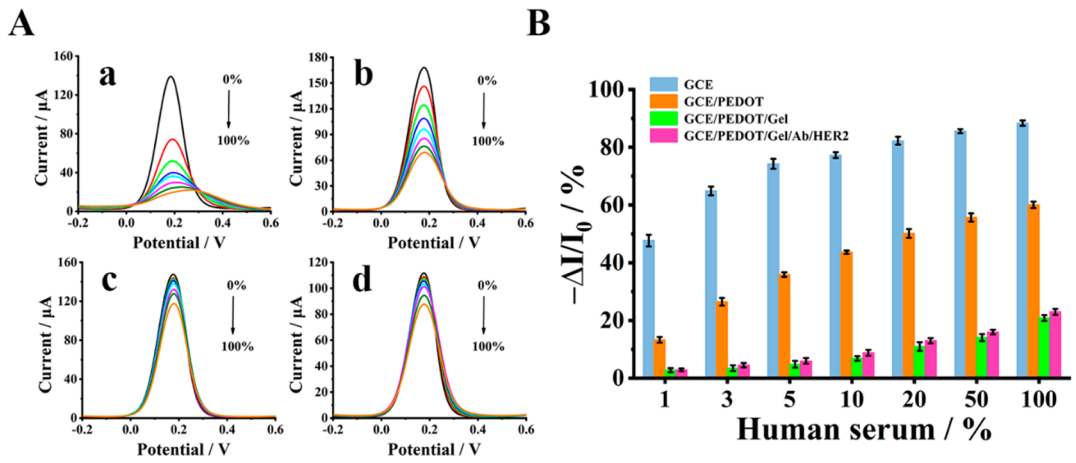

Figure 5. (A) DPV responses of (a) bare GCE, (b) GCE/PEDOT, (c) GCE/PEDOT/gel, and (d) GCE/PEDOT/Gel/Ab/HER2 after incubation in human sera with different concentrations. (B) The corresponding signal change rates of different electrodes. Error bars show the standard deviations of three repeated measurements.

https://doi.org/10.1021/acs.analchem.1c01350
Anal. Chem. 2021, 93, 7355−7361

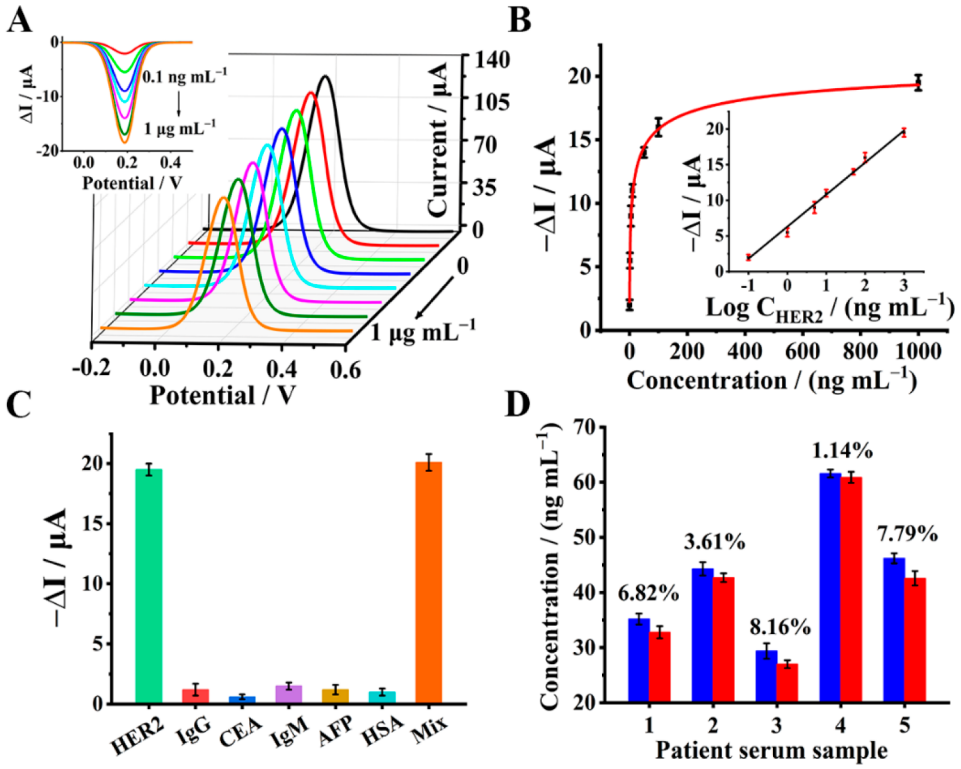

Figure 6. (A) DPV responses of the HER2 biosensor after incubation in HER2 for a range of concentrations. Inset: DPV responses after background removal. (B) Corresponding response signal change of the HER2 biosensor. Inset: calibration curve of the HER2 biosensor. (C) Responses of the HER2 biosensor to 0.1 mg mL^{-1} of IgG, CEA, IgM, AFP, HSA and a solution mixture (Mix) of those proteins, respectively. (D) HER2 determination of breast cancer patient serum utilizing a commercial ELISA Kit (blue) and the developed biosensor (red). Error bars show the standard deviations of three repeated measurements.

This result demonstrated that the constructed HER2 biosensor possessed an excellent accuracy and was suitable for HER2 detection in real samples.

CONCLUSIONS

In short, a novel, ultrasensitive, and antifouling electrochemical biosensor for the detection of the breast cancer biomarker HER2 was constructed on the basis of the integration of peptide hydrogels with the stable conducting polymer PEDOT. The nanofibrous network structure, high hydrophilicity, and brilliant biocompatibility of the hydrogels enabled the activity of the immobilized biomolecules to be retained and the formation of a hydration barrier for fouling alleviation, making them an ideal candidate for biosensor fabrication. Notably, the prepared electrochemical immunosensor was capable of detecting HER2 in real serum samples with acceptable accuracy and also exhibited a wide detection range, low LOD, and desirable selectivity, showing a bright prospect in bioanalysis and clinical diagnosis.

ASSOCIATED CONTENT

Supporting Information

The Supporting Information is available free of charge at https://pubs.acs.org/doi/10.1021/acs.analchem.1c01350.

SEM characterization, static water contact angle measurements, long-term antifouling characterization, optimization of experimental conditions, and stability and reproducibility of the biosensor (PDF)

AUTHOR INFORMATION

Corresponding Author

Xiliang Luo − *Key Laboratory of Optic-electric Sensing and Analytical Chemistry for Life Science, MOE, Shandong Key Laboratory of Biochemical Analysis, Key Laboratory of Analytical Chemistry for Life Science in Universities of Shandong, College of Chemistry and Molecular Engineering, Qingdao University of Science and Technology, Qingdao 266042, People's Republic of China;* orcid.org/0000-0001-6075-7089; Phone: +86 532 84022860; Email: xiliangluo@qust.edu.cn; Fax: +86 532 84022681

Authors

Wenqi Wang − *Key Laboratory of Optic-electric Sensing and Analytical Chemistry for Life Science, MOE, Shandong Key Laboratory of Biochemical Analysis, Key Laboratory of Analytical Chemistry for Life Science in Universities of Shandong, College of Chemistry and Molecular Engineering, Qingdao University of Science and Technology, Qingdao 266042, People's Republic of China*

Rui Han − *Key Laboratory of Optic-electric Sensing and Analytical Chemistry for Life Science, MOE, Shandong Key Laboratory of Biochemical Analysis, Key Laboratory of Analytical Chemistry for Life Science in Universities of Shandong, College of Chemistry and Molecular Engineering, Qingdao University of Science and Technology, Qingdao 266042, People's Republic of China*

Min Chen − *Key Laboratory of Optic-electric Sensing and Analytical Chemistry for Life Science, MOE, Shandong Key Laboratory of Biochemical Analysis, Key Laboratory of*

https://doi.org/10.1021/acs.analchem.1c01350
Anal. Chem. 2021, 93, 7355−7361

Analytical Chemistry for Life Science in Universities of Shandong, College of Chemistry and Molecular Engineering, Qingdao University of Science and Technology, Qingdao 266042, People's Republic of China

Complete contact information is available at: https://pubs.acs.org/10.1021/acs.analchem.1c01350

Notes

The authors declare no competing financial interest.

■ ACKNOWLEDGMENTS

This work was supported in part by the National Natural Science Foundation of China (21974075), the Science and Technology Benefiting the People Project of Qingdao (20-3-4-53 nsh), and the Taishan Scholar Program of Shandong Province of China (ts20110829).

■ REFERENCES

(1) Li, Z.; Wang, Y.; Wang, J.; Tang, Z.; Pounds, J. G.; Lin, Y. *Anal. Chem.* **2010**, *82* (16), 7008−7014.
(2) Sawyers, C. L. *Nature* **2008**, *452* (7187), 548−552.
(3) Wu, L.; Qu, X. *Chem. Soc. Rev.* **2015**, *44* (10), 2963−2997.
(4) Luo, X.; Davis, J. J. *Chem. Soc. Rev.* **2013**, *42* (13), 5944−5962.
(5) Labib, M.; Sargent, E. H.; Kelley, S. O. *Chem. Rev.* **2016**, *116* (16), 9001−9090.
(6) Gunkel, G.; Huck, W. T. S. *J. Am. Chem. Soc.* **2013**, *135* (18), 7047−7052.
(7) Wang, G.; Han, R.; Li, Q.; Han, Y.; Luo, X. *Anal. Chem.* **2020**, *92* (10), 7186−7193.
(8) Song, Z.; Chen, M.; Ding, C. F.; Luo, X. L. *Anal. Chem.* **2020**, *92* (8), 5795−5802.
(9) Liu, B.; Liu, X.; Shi, S.; Huang, R.; Su, R.; Qi, W.; He, Z. *Acta Biomater.* **2016**, *40*, 100−118.
(10) Vaisocherová, H.; Brynda, E.; Homola, J. *Anal. Bioanal. Chem.* **2015**, *407* (14), 3927−3953.
(11) Makamba, H.; Hsieh, Y. Y.; Sung, W. C.; Chen, S. H. *Anal. Chem.* **2005**, *77* (13), 3971−3978.
(12) Liu, N. Z.; Song, J. Y.; Lu, Y. W.; Davis, J. J.; Gao, F. X.; Luo, X. L. *Anal. Chem.* **2019**, *91* (13), 8334−8340.
(13) Bengani-Lutz, P.; Converse, E.; Cebe, P.; Asatekin, A. *ACS Appl. Mater. Interfaces* **2017**, *9* (24), 20859−20872.
(14) Patel, J.; Radhakrishnan, L.; Zhao, B.; Uppalapati, B.; Daniels, R. C.; Ward, K. R.; Collinson, M. M. *Anal. Chem.* **2013**, *85* (23), 11610−11618.
(15) Banerjee, I.; Pangule, R. C.; Kane, R. S. *Adv. Mater.* **2011**, *23* (6), 690−718.
(16) Jiang, C.; Wang, G. X.; Hein, R.; Liu, N. Z.; Luo, X. L.; Davis, J. J. *Chem. Rev.* **2020**, *120* (8), 3852−3889.
(17) Frost, M.; Meyerhoff, M. E. *Anal. Chem.* **2006**, *78* (21), 7370−7377.
(18) Lowe, S.; O'Brien-Simpson, N. M.; Connal, L. A. *Polym. Chem.* **2015**, *6* (2), 198−212.
(19) Emilsson, G.; Schoch, R. L.; Feuz, L.; Höök, F.; Lim, R. Y. H.; Dahlin, A. B. *ACS Appl. Mater. Interfaces* **2015**, *7* (14), 7505−7515.
(20) He, S. B.; Wu, G. W.; Deng, H. H.; Liu, A. L.; Lin, X. H.; Xia, X. H.; Chen, W. *Biosens. Bioelectron.* **2014**, *62*, 331−336.
(21) Huang, R.; Liu, X.; Ye, H.; Su, R.; Qi, W.; Wang, L.; He, Z. *Langmuir* **2015**, *31* (44), 12061−12070.
(22) Jolly, P.; Formisano, N.; Tkáč, J.; Kasák, P.; Frost, C. G.; Estrela, P. *Sens. Actuators, B* **2015**, *209*, 306−312.
(23) Ham, H. O.; Park, S. H.; Kurutz, J. W.; Szleifer, I. G.; Messersmith, P. B. *J. Am. Chem. Soc.* **2013**, *135* (35), 13015−13022.
(24) Wang, G.; Han, R.; Su, X.; Li, Y.; Xu, G.; Luo, X. *Biosens. Bioelectron.* **2017**, *92*, 396−401.
(25) Dou, X. Q.; Feng, C. L. *Adv. Mater.* **2017**, *29* (16), 1604062.
(26) Wang, J. H.; Chen, X. Y.; Zhao, Y.; Yang, Y. M.; Wang, W. J.; Wu, C.; Yang, B. Z.; Zhang, Z. T.; Zhang, L. S.; Liu, Y.; Du, X. C.; Li, W. F.; Qiu, L.; Jiang, P. J.; Mou, X. Z.; Li, Y. Q. *ACS Nano* **2019**, *13* (10), 11686−11697.
(27) Chakraborty, P.; Guterman, T.; Adadi, N.; Yadid, M.; Brosh, T.; Adler-Abramovich, L.; Dvir, T.; Gazit, E. *ACS Nano* **2019**, *13* (1), 163−175.
(28) Zhang, F. J.; Hu, C.; Kong, Q. S.; Luo, R. F.; Wang, Y. B. *ACS Appl. Mater. Interfaces* **2019**, *11* (40), 37147−37155.
(29) Lian, M.; Chen, X.; Lu, Y.; Yang, W. *ACS Appl. Mater. Interfaces* **2016**, *8* (38), 25036−25042.
(30) Adak, A.; Das, G.; Barman, S.; Mohapatra, S.; Bhunia, D.; Jana, B.; Ghosh, S. *ACS Appl. Mater. Interfaces* **2017**, *9* (6), 5067−5076.
(31) George, S. M.; Tandon, S.; Kandasubramanian, B. *ACS OMEGA* **2020**, *5* (5), 2060−2068.
(32) Wu, J. G.; Chen, J. H.; Liu, K. T.; Luo, S. C. *ACS Appl. Mater. Interfaces* **2019**, *11*, 21294−21307.
(33) Liu, N. Z.; Xu, Z. Y.; Morrin, A.; Luo, X. L. *Anal. Methods* **2019**, *11* (24), 702−711.
(34) Li, X. Q.; Shen, C. C.; Yang, M. H.; Rasooly, A. *Anal. Chem.* **2018**, *90* (7), 4764−4769.
(35) Campone, M.; De Laurentiis, M.; Zamagni, C.; Kudryavcev, I.; Agterof, M.; Brown-Glaberman, U.; Palácová, M.; Chatterjee, S.; Menon-Singh, L.; Wu, J.; Zhou, K.; Martin, M. *Ann. Oncol.* **2019**, *30*, No. v115.
(36) Scaltriti, M.; Rojo, F.; Ocaña, A.; Anido, J.; Guzman, M.; Cortes, J.; Di Cosimo, S.; Matias-Guiu, X.; Ramon y Cajal, S.; Arribas, J.; Baselga, J. *JNCI-J. Natl. Cancer Inst.* **2007**, *99* (8), 628−638.
(37) Gangopadhyay, R.; De, A. *Chem. Mater.* **2000**, *12* (3), 608−622.
(38) Hui, N.; Sun, X.; Niu, S.; Luo, X. *ACS Appl. Mater. Interfaces* **2017**, *9* (3), 2914−2923.
(39) Oh, W. K.; Kwon, O. S.; Jang, J. *Polym. Rev.* **2013**, *53* (3), 407−442.
(40) Basavalingappa, V.; Guterman, T.; Tang, Y.; Nir, S.; Lei, J.; Chakraborty, P.; Schnaider, L.; Reches, M.; Wei, G.; Gazit, E. *Adv. Sci. (Weinh)* **2019**, *6* (12), 1900218.
(41) Wang, W.; Han, R.; Tang, K.; Zhao, S.; Ding, C.; Luo, X. *Anal. Chim. Acta* **2021**, *1154*, 338295.
(42) Feng, T.; Ji, W.; Tang, Q.; Wei, H.; Zhang, S.; Mao, J.; Zhang, Y.; Mao, L.; Zhang, M. *Anal. Chem.* **2019**, *91* (16), 10786−10791.
(43) Tang, L.; Thevenot, P.; Hu, W. *Curr. Top. Med. Chem.* **2008**, *8* (4), 270−280.
(44) Hanssen, B. L.; Siraj, S.; Wong, D. K. Y. *Rev. Anal. Chem.* **2016**, *35* (1), 1−28.